



**HAL**  
open science

## **New VMD2 gene mutations identified in patients affected by Best vitelliform macular dystrophy**

D Marchant, Y. Kuai, O Roche, A Germain, D Bonneau, D Schorderet, D Schmidt, P Le Neindre, C Marsac, M Menasche, et al.

### ► **To cite this version:**

D Marchant, Y. Kuai, O Roche, A Germain, D Bonneau, et al.. New VMD2 gene mutations identified in patients affected by Best vitelliform macular dystrophy. *Journal of Medical Genetics*, 2007, 44 (3), pp.e70-e70. 10.1136/jmg.2006.044511 . hal-02942101

**HAL Id: hal-02942101**

**<https://hal.science/hal-02942101>**

Submitted on 27 Feb 2021

**HAL** is a multi-disciplinary open access archive for the deposit and dissemination of scientific research documents, whether they are published or not. The documents may come from teaching and research institutions in France or abroad, or from public or private research centers.

L'archive ouverte pluridisciplinaire **HAL**, est destinée au dépôt et à la diffusion de documents scientifiques de niveau recherche, publiés ou non, émanant des établissements d'enseignement et de recherche français ou étrangers, des laboratoires publics ou privés.

# **New VMD2 gene mutations identified in patients affected by Best's Vitelliform Macular Dystrophy.**

**D. Marchant<sup>1</sup>, Y. Kuai<sup>4</sup>, O. Roche<sup>2</sup>, A. Germain<sup>1</sup>, D. Bonneau, D. F. Schorderet<sup>3</sup>, Danielle Schmidt<sup>2</sup>, P Le Neindre<sup>2</sup>, C. Marsac<sup>1</sup>, M. Menasche<sup>1</sup>, J.L. Dufier<sup>2</sup>, R. Fischmeister<sup>5</sup>, H. Criss. Hartzell<sup>4\*</sup> and M. Abitbol<sup>1\*</sup>.**

*1 Centre de recherche thérapeutique en ophtalmologie, équipe d'accueil 2502 MENRT, Université René Descartes Paris V, Faculté de Médecine Necker-Enfants Malades, 156 rue de Vaugirard, 75015 Paris, France.*

*2 Département d'ophtalmologie, Centre Hospitalier Universitaire Necker-Enfants Malades, 149 rue de Sèvres, 75015 Paris, France*

*3 Division de Génétique Médicale, Centre Hospitalier Universitaire Vaudois, Lausanne, Switzerland.*

*4 Department of Cell Biology, The Center for Neurodegenerative Disease, Emory University School of Medicine, Atlanta, Georgia, USA*

*<sup>5</sup> INSERM U769, Châtenay-Malabry, F-92296 France*

*\*Correspondence and reprint request: Dr Marc Abitbol, Centre de recherche thérapeutique en ophtalmologie, Université René Descartes Paris V, Faculté de Médecine Necker-Enfants Malades, 156 rue de Vaugirard, 75015 Paris, France; Dr. Criss Hartzell Department of Cell Biology, The Center for Neurodegenerative Disease, Emory University School of Medicine, Atlanta, Georgia, USA*

E-mail : abitbol@necker.fr ; Tel. : (+33) 01.40.61.56.57 ; Fax. : (+33) 01.40.61.54.74

criss.hartzell@emory.edu ; Tel.: (+1) 404 727 0444; Fax. : (+1) 404 727 6256

Short Title: New VMD2 gene mutations

**Abstract** The *VMD2* gene encodes a transmembrane protein named bestrophin-1 which is a Ca<sup>2+</sup>-sensitive chloride channel. Here, we identified six new *VMD2* mutations in patients with Best's macular dystrophy. One of these mutations (Q293H) is particularly severe. Patch clamp analysis of HEK cells expressing the Q293H mutant shows that this mutant channel is non-functional. Furthermore, the Q293H mutant inhibits the function of wild-type bestrophin-1 channels in a dominant negative manner. Direct sequencing analysis of the 11 *VMD2* exons revealed new abnormal profiles in exons 4, 6 and 8 due to mono-allelic transitions and transversions. We also detected five frequent pathogenic sequence changes that have been previously reported and annotated in an online database.

(<http://www.uni-wuerzburg.de/humangenetics/vmd2.html>)

**Key words:** Best's macular dystrophy, *VMD2* (OMIM 153700), chloride channel

## INTRODUCTION

Best's disease, also called Best's Vitelliform Macular Dystrophy (BVMD), is a bilateral, symmetric, progressive disease of the retinal pigment epithelium (RPE) of the macular area leading to loss of vision. It has an autosomally dominant transmission, but the penetrance is incomplete and its expression is highly variable (1-3). Although it is the second most common form of juvenile macular degeneration, with an onset usually before 15 years of age, only about 1% of all cases of macular degeneration can be attributed to Best's disease (reference).

On fundus examination, the central macula takes on an "egg yolk"-like appearance. This lesion is a large abnormal accumulation of yellow lipofuscin pigment within and beneath the RPE. At this stage, visual acuity is surprisingly good (20/20). The lesions are often bilateral, measuring between one and two disc areas in size. About 10% of affected eyes have multifocal lesions in the extrafoveal region. The lesion evolves through several stages over many years, with visual acuity usually decreasing in later life (visual acuity does not decrease until the yolk-like lesion "scrambles," becoming pigmented and irregular in appearance). The lesion may degenerate, resulting in macular choroidal neovascularisation, haemorrhage and scarring. In the scarred state, it may be indistinguishable from age-related macular degeneration (ARMD). The degree of central vision impairment and the age of onset of symptoms varies widely, even among members of the same family. Some people who carry causative BVMD mutations may never experience a noticeable decline of central vision. Dark adaptation is usually normal.

During angiographic examination, the vitelliform lesion typically results in hypofluorescence due to the underlying choroidal fluorescence being blocked and the overlying retinal vasculature being visible (references). This means the lesion is in front of the choroid and within and beneath the RPE, but not within the neural retina. Lesions similar to those seen in Best's disease may occur in patients with pseudo vitelliform or adult vitelliform macular

degeneration (AVMD) (reference). In some cases, similar conditions are caused by mutations of other genes.

The differential diagnosis of BVMD from other macular dystrophies is most effectively made by measuring the electro-oculogram (EOG) (4), whereas full-field electroretinograms (ERGs) are usually normal in BVMD patients (1,2,5,6). In both affected patients and carrier patients, EOG shows an abnormal light-peak / dark-trough ratio in the EOG. Abnormal EOG responses can be recorded in asymptomatic patients, sometimes long before the appearance of any clinical manifestations. Multifocal electroretinography (mERG) reveals variable central function loss depending on the stage of the disease and has become an important tool in assessing the function of the remaining macular cones (5-7). Optical coherent tomography (OCT) allows the non-invasive evaluation of the lipofuscin deposit in the RPE and has also become an important tool in examining the lesions of the macula. EOG, mERG and OCT are now used to establish diagnosis and to assess the prognosis of Best's disease affected patients.

The mutations responsible for Best's disease are found in a gene called *VMD2*. It encodes a transmembrane protein named bestrophin-1 (hBest1). The protein is located in the basolateral plasma membrane of RPE cells (8). Bestrophin is a member of the RFP-TM family of proteins, so named for their highly conserved arginine, phenylalanine, proline (RFP) motif (9-11). Bestrophin contains several domains that are highly conserved between species (9). Patch-clamp studies of bestrophin and other RFP-TM family members heterologously overexpressed in cell culture have suggested that bestrophin is a Ca<sup>2+</sup>-sensitive chloride channel (12-14).

Some mutations in the *VMD2* gene have also been associated with some cases of bull's-eye maculopathy (15) and of AVMD (15-18).

In this study, we identify six new, independent, disease-specific mutations in BVMD patients and their families, and in isolated patients. One of these mutations (Q293H) found in a large family from the west part of France, Q293H is particularly severe. Patch clamp analysis of

HEK cells expressing the Q293H mutant bestrophin-1 shows that this mutant channel is non-functional. Furthermore, the Q293H mutant inhibits the function of wild-type bestrophin-1 channels in a dominant negative manner. These findings support the idea that BVMD is a chloride channelopathy.

## **MATERIALS AND METHODS**

### **Patients**

Informed consent was obtained from all study participants. Of the 27 BVMD probands, 25 were from France (eight families (B to I) and six isolated patients (a to f)), and two were **from the French-speaking part of Switzerland (Canton de Vaud) (families A and J) (Table 1)**. The control group consisted of 100 unrelated individuals from France who were unaffected by any of form of macular degeneration or inherited retinal dystrophy and who had no family history of BVMD (as described by Marchant *et al.*, (19)).

### **The clinical diagnosis of Best's disease:**

The clinical diagnosis of Best disease was based on one or multiple subfoveal vitelliform lesions in at least one eye. At least one affected individual from each family was diagnosed by both electro-oculography (EOG) and fundus examination. The hallmark diagnostic feature of Best's disease is the decreased slow light peak in the EOG. The EOG provides information about the function of the retinal pigment epithelium. During dark adaptation, the resting potential decreases slightly, reaching a minimum ("dark trough") after several minutes. When the light is switched on, there is a large increase in the resting potential ("light peak"), which decreases after several minutes as the retina adapts to the light. The ratio of the two voltages (i.e. the light peak divided by the dark trough) is known as the Arden ratio (references).

In addition, families C and I were also evaluated by multifocal electroretinography (mERG) and optical coherence tomography (OCT) analysis. OCT images retinal structures in real-time on the micron scale (20-22) and gives high-resolution, cross-sectional tomographic images of the internal microstructure of materials and biological systems by measuring backscattered or back-reflected light. Electroretinography is used to measure the electrical responses of various cell types within the outer retina, such as the light-sensitive rods and cones, Müller cells, and bipolar cells. Conventional full-field ERGs are often reported to be normal in Best's disease (references). Very rare ERG abnormalities can sometimes be seen, but these probably reflect degenerative changes secondary to the initial vitelliform lesions. mERG uses multiple electrodes to stimulate each visual field location. Due to the independent nature of the stimulus sequence, the responses for each visual field location can be extracted using mathematical algorithms. Thus, mERG allows spatial differences in retinal function to be determined, usually revealing reductions in the central amplitude of patients with clinical symptoms (23).

### **VMD2 gene analysis**

Genomic DNA was extracted from all study participants from venous blood using a standard proteinase K extraction protocol (reference). hBest1 consists of 11 exons. Each exon with short flanking intronic sequence at both the 5' and 3' ends was from all 79 BVMD patients and 100 controls using touch-down PCR (reference) with oligonucleotide primers designed to intronic sequence flanking the exon. (the primers used and the PCR cycling conditions are available on request). DNA was then bi-directionally sequenced using an automated sequencer and dye-terminator chemistry (ABI Prism DNA 310 machine). We used ESEfinder© software (<http://exon.cshl.edu/ESE/>) to search for putative ESE motifs (24).

### **Functional analysis of variant in HEK cells**

### Site-specific mutagenesis of hBest1 and heterologous expression in mammalian cell lines

Point mutations were made in human Bestrophin-1 (hBest1) using a PCR-based site directed mutagenesis kit (Quickchange; Stratagene), as previously described (25). Wild type hBest1 cDNA in pRK5 was kindly provided by Dr. Jeremy Nathans (Johns Hopkins University). HEK-293 cells (human embryonic kidney, ATCC) were co-transfected with hBest1 cDNA and a vector expressing EGFP (pEGFP; Invitrogen) using Fugene-6 transfection reagent (Roche). We transfected the cells of one 35 mm culture dish with 1  $\mu$ g hBest1 cDNA to obtain a modest  $\text{Ca}^{2+}$ -activated  $\text{Cl}^-$  current (1 to 2 nA per cell). One day after transfection, cells were dissociated and replated on glass coverslips for electrophysiological recording. Transfected cells were identified by EGFP fluorescence and used for patch clamp experiments within three days of transfection.

### Electrophysiology

Whole cell patch clamp recording was done essentially as described by Qu *et al.* (25). Briefly, Patch pipettes (2–3.5  $\text{M}\Omega$  filled with the standard intracellular solution) were made of borosilicate glass (Sutter Instrument Co.), pulled by a Sutter P-2000 puller (Sutter Instrument Co.), and fire polished. The bath was grounded via a 3 M KCl agar bridge connected to a Ag/AgCl reference electrode. Solution changes were performed by perfusing the 1-ml chamber at a speed of  $\sim 4$  ml/min. Data were acquired by an Axopatch 200A amplifier controlled by Clampex 8.1 via a Digidata 1322A data acquisition system (Axon Instruments). Experiments were conducted at room temperature (20–24°C). The standard pipette solution contained (in mM) 146 CsCl, 2  $\text{MgCl}_2$ , 5 ( $\text{Ca}^{2+}$ )-EGTA, 8 HEPES, 10 sucrose, pH 7.3, adjusted with NMDG. The free  $[\text{Ca}^{2+}]$  in the high  $\text{Ca}^{2+}$  solution was  $\sim 5$   $\mu\text{M}$ . The standard extracellular solution contained (in mM) 140 NaCl, 5 KCl, 2  $\text{CaCl}_2$ , 1  $\text{MgCl}_2$ , 15 glucose, 10 HEPES, pH 7.3 with NaOH. This combination of solutions set the reversal potential ( $E_{\text{rev}}$ ) for  $\text{Cl}^-$  currents to zero, while cation currents carried by  $\text{Na}^+$  or  $\text{Cs}^+$  have very positive or negative  $E_{\text{rev}}$ , respectively.

## RESULTS

Most of the BVMD-affected patients included in our study presented a classical BVMD phenotype with bilateral “egg yolk”-like deposits observed fundoscopically, with a significant bilateral decrease of the Arden ratio on EOG examination. OCT also detected abnormal lipofuscin deposits and abnormal retinal structures in the macular region. In addition, alterations in the mERG was observed in most of the patients. The mERG alterations usually correlated well with either the decrease in visual acuity or, if visual acuity was preserved, with central scotomas detected by visual field examination.

Family C presented noticeable exceptions to this phenotype. Nearly all affected individuals in this family were diagnosed at a very early age: about six years of age with typical vitelliform lesions already visible in fundoscopic examination and EOG alterations. The visual acuity of most of these patients decreased considerably at about ten years of age to 2/20. Several of these patients developed very early foveal neovascular lesions, which led to a haemorrhagic retinal macular detachment in one case. Patient IV-5, the initial proband of this study, presented the typical severe phenotype that affects this family, with a typical fundoscopic appearance at about five years of age. A rapid evolution of the visible lesion was observed, with a bilateral enlargement of the “egg yolk” deposit occurring first, followed by visible fragmentation of the right eye lesion accompanied by a very marked unilateral decrease in visual acuity. This evolution was associated with a decreased Arden ratio. We were unable to carry out OCT and mERG on this patient due to an understandable lack of cooperation at this age. BVMD also started at a very young age (five years of age) in patient III-2. At 13 years of age, the patient experienced an acute bilateral decrease in his visual acuity associated with a rapid decrease in the Arden ratio with the development of foveolar choroidal neovessels being clearly visible by fluorescein angiography (Fig 1). We have recently been able to examine the patient, who is now 34 years of age. His EOG showed low basic values and an Arden ratio of 1.1 for both eyes. The ERG showed a normal

response of the cones and rods, and a normal response to flicker. The oscillatory potentials were also normal. **mERG** revealed a symmetrical response of the two eyes. However, we observed a noticeably altered retinal electrogenesis of the central cones, with a lowered foveal peak crest and some **parafoveal** defects. OCT examination revealed abnormal lipofuscin deposits in the central macular area and an abnormal structure of the central retina. We also examined patient II-1, who had transmitted BVMD to patient III-2, his son. Like his son, patient II-1 had a loss of vision at a very young age. His eyes had not been previously examined before we met him. He was 71 years of age with a visual acuity of 20/200 for the right eye and 40/200 for the left eye. Fundoscopy **revealed** a bilateral atrophy of the central macula with telangiectasia of the perimacular capillary network. EOG examination showed a symmetrical response of the two eyes. The basic values were low and the Arden ratio was pathologically close to extinction (Arden ratio= 1.1). **mERG** showed a symmetrical response of the two eyes. The retinal electrogenesis of the central cones was severely altered. Foveal peaks had disappeared and we detected disseminated macular decreases of mERG local amplitudes, corresponding to foveal scotomas. OCT examination revealed lipofuscin deposits in the foveal area for both eyes, although there were more deposits in the macular area of the left eye. The disease was much more progressive in the right eye. Choroidal neovessel development was so extensive in this eye that it was associated with a neuroretinal schisis.

Although the phenotype of family C is especially severe, the general pattern of incomplete penetrance and variable expressivity could be seen among different members of this pedigree carrying the same mutation. Indeed, patient III-8 (the father of IV-5) is 35 years of age and had a visual acuity of 20/20 for each eye. Fundoscopy and fluorescein angiography were normal for each eye. However, he had a severely altered EOG (Arden ratio=1) for both eyes, whereas **OCT examination and mERG were completely normal.**

## Genetic analysis

For each BVMD patient, we found only one mutation in the coding sequence of *VMD2*. Among these mutations, five have previously been reported to be common BVMD mutations (reference), but six are novel mutations that have not previously been reported. All of the mutations were missense mutations. These were mainly located in exons four, six and eight. Five of the six new mutations (G222E, S231T, P233Q, Q293h and G299R) are located within regions known to be affected by frequent mutations (“hotspot” regions). None of these changes were found in the 100 control individuals. The mutations are summarized in Table 1. **All mutations were found to co-segregate with the disease in all symptomatically affected family members. The mutations were usually absent in the unaffected family members.**

According to Nathan’s model of human bestrophin (hBest1) topology (13), the new missense L134V mutation found in exon four is located between the second (TM2) and the third (TM3) putative transmembrane domain of bestrophin. This mutation does not substantially change the electric charge or the nature of the amino-acid, and therefore it is not obvious how this modification leads to BVMD. However, the same type of mutation has been previously described in a BVMD patient and was considered a pathogenic alteration (L294V) (26). Leucine is completely conserved at position 134 in the bestrophin-related family members (*VMD2L1*, *VMD2L2* and *VMD2L3*) suggesting that it plays an important functional or structural role. The Leu104 residue is also highly conserved among other species, including **nematodes** (9). **Therefore, this substitution is likely to be a pathogenic mutation.**

We found three new missense mutations in exon six (G222E, S231T and P233Q). These amino acids are located between TM2 and TM3. Gly222 is only conserved in human *VMD2L1* whereas Ser231 is conserved in *VMD2L1* and *VMD2L2*. The Pro233 residue is invariant within the entire human *VMD2*-like protein family and within phylogenetically distant bestrophin orthologues.

Two new mutations (Q293H and G299R) are located in exon 8 of *VMD2*, in the fourth defined hotspot region, and after the fourth putative transmembrane (TM4) domain of bestrophin (26). Gln293 and Gly299 are invariant in human *VMD2L1*, *VMD2L2* and *VMD2L3* (11). Gly299 is also highly conserved within RFP family members. **The Q293H mutation co-segregated with the disease in all the members of family C who had symptoms of Best disease and none of the clinically unaffected members of family C carried the Q293H mutation. The Q293H mutation, however, exhibited incomplete penetrance because patient III-8 had an extinguished EOG but had normal visual acuity and a normal fundoscopic examination.**

We also found six frequent polymorphisms in the affected BVMD patients, as well as in the related unaffected BMD patients and in the 100 control individuals (see Table 2). These polymorphisms did not alter the predicted amino acid sequence of the bestrophin protein (Table 2). These apparently silent nucleotide variations were found in many of the studied patients, either as a homozygous or a heterozygous substitution.

### **Functional analysis of Q293H variant in HEK cells**

To test the hypothesis that the Q293H mutation produces Best disease because it alters Cl<sup>-</sup> channel function, we expressed the Q293H mutant of hBest1 in HEK-293 cells and examined associated Cl<sup>-</sup> current using whole-cell patch clamp (14,25,27,28). Fig. 2A shows the Cl<sup>-</sup> currents in HEK-293 cells associated with expression of hBest1 wild type cDNA as we have previously reported (Fisch & Hartzell). The currents are time- and voltage-independent. The current-voltage relationship is essentially linear (Fig. 2D). Fig. 2B shows the currents produced by the Q293H mutation. The currents are extremely small and cannot be clearly differentiated from the endogenous Cl<sup>-</sup> currents in HEK-293 cells. The Q293H mutation is essentially non-functional. Some bestrophin mutations have been shown to behave as dominant negatives: co-expression of the mutant bestrophin with the wild-type causes a reduction or elimination of the wild type current

(references). Because disease is inherited in a dominant manner with the Q293H mutation, one might expect that this mutation is also a dominant negative. To test this possibility, the Q293H mutant was co-expressed with wild type hBest1. The currents obtained from cells co-expressing wild type and Q293H hBest1 had currents that were reduced significantly in amplitude to those cells expressing hBest1 wild type alone (Fig. 2C and 2E). On average, the current amplitude with wild type and Q293H expressed together was less than half that of the wild type alone. Thus, Q293H has a dominant negative effect. The reason why the Q293H mutation does not completely abolish the wild type current could be related to differences in expression levels of the two constructs.

## DISCUSSION

In this **report**, we describe six new mutations and five frequent pathogenic sequence changes in a phenotypically homogeneous sample of patients and families affected by BVMD. We identified these mutations in the *VMD2* gene by examining all 11 exons and their boundaries in the *VMD2* gene in 39 individuals from 11 families and six isolated cases. We detected *VMD2* mutations in all of the isolated clinically-diagnosed BVMD cases with no family history of Best disease as well as in individuals in families having a positive familial history of Best disease. Thus, **these studies provide further support to the idea that mutations in hBest1 are a necessary factor for Best disease.**

However, it is also clear that a disease-linked mutation in hBest1 is not sufficient to produce the disease: there must be other factors involved. This is shown clearly by the incomplete penetrance of *VMD2* observed in family C which carries the Q293H mutation. It may be that a high level of expression of the wild-type allele may be compensating for the mutant allele, as suggested by McGee *et al* (30). There may be **variable** regulatory regions within the *VMD2* promoter sequence that modulate the level of expression of the wild type allele relative to the mutant allele. Esumi *et al.* have identified two positive regulatory regions in the *VMD2* promoter

sequence, from -585 to -541 bp for high level expression and -56 to -42 bp for low level expression (32). They also suggested that E-box binding factors such as MITF may act as positive regulators of *VMD2* expression. Therefore, we cannot exclude a nucleotide change, possibly corresponding to an SNP in the promoter sequence, as causing the incomplete penetrance and the variability of *VMD2* expression between the asymptomatic patient (III-6) and the BVMD-affected patients in family C. Another possibility is that polymorphisms in the wild type allele compensate for the defect in the mutant allele. Such an allelic effect was suggested for the non-penetrance of mutations at the *RP11* locus. Vithana *et al.* showed that asymptomatic patients with autosomal dominant retinitis pigmentosa (RP11) inherit a different wild-type allele of the *PRPF31* gene **to that** inherited by symptomatic patients (31).

The predicted hBest1 topology described by Hartzell *et al* (28) shows that the amino acid mutations we have identified were probably located either in an extracellular loop or the C-terminal cytoplasmic tail. The exact location of Q293H remains in question, because it is near the end of the last transmembrane domain and could be located in the plasma membrane, at its interface, or in the cytoplasm. Q293 is not accessible to the extracellular aqueous environment because when it is replaced with cysteine, it is apparently not modified by membrane-impermeant sulfhydryl reagents (Tsunenari *et al.* ). Q293 is the first residue in a string of 18 amino acids (293 - 311), 16 of which have been shown to be linked to Best disease when mutated. These findings clearly pinpoint this as an important region. Its exact function, however, remains unknown. The high concentration of acidic amino acids might be a Ca binding site or a protein trafficking signal, both of which often have a negative charge. Our finding that the Q293H mutant does not form functional channels in the membrane could be explained either by disruption of channel conductance or gating mechanisms or by improper trafficking of the protein to the plasma membrane.

Sun *et al.* (12) have previously shown that certain hBest1 mutations induce smaller whole-cell currents than does wild type hBest1 when expressed in HEK-293 cells. Three of the mutations they studied occur at the same positions as three of the mutations we have identified (R218S, Q293K and G299E), but the substituted amino acid is different (R218C/H, Q293H and G299R). They found that amplitude of the current induced by the Q293K mutation was 25% that of the wild type current. We find that the Q293H mutation produces no current whatsoever. This may be consistent with the very severe nature of the Q293H disease.

Our data adds several more examples of amino acids that produce Best disease when mutated to different amino acids. For example, R218 was substituted with cysteine in one family and histidine in another. Furthermore, as noted above, Q293, G299, and R218 have multiple disease-associated mutations. Each of the affected families or isolated cases had a unique mutation. However, we found some mutations in several unrelated families and isolated patients. We identified the R218C mutation twice in unrelated families and isolated cases and the R218H mutation four times in unrelated families and isolated cases. If we include the data from our previous studies (19,29), the most commonly affected amino acid residue in the French families and isolated patients affected by Best disease is R218 (8 alleles). Indeed, the R218C and R218H mutations were the most common and may correspond to a founder effect in the French population and other western populations. The other commonly altered amino acid residues may be mutation hotspots and/or functionally important protein residues.

The detection rate for mutations in *VMD2* is high in Best's disease patients irrespective of the method used for the genetic analysis (direct DNA sequencing of PCR-amplified exons or single stranded conformational polymorphism, or denaturing HPLC). However, the location of the mutation means that difficulties can be encountered in detecting pathogenic mutations in BVMD patients (10,29,33,34). PCR amplification of individual exons may miss large deletions, rearrangements or mutations affecting 5' or 3' untranslated regions, or mutations within the

promoter sequence or within the intronic sequence, which can generate new splice sites. Real-time quantitative PCR of the entire *VMD2* gene should allow monochromosomal deletions or duplications to be detected, which can be missed by direct sequencing and Southern blotting. RT-PCR can be used to detect illegitimate transcription in total RNA extracted from lymphoblastoid cell lines or from white blood cells, allowing the identification of aberrant transcripts due to abnormal alternative splicing events.

## **ACKNOWLEDGMENTS**

We thank all the patients for their cooperation in this study. This work was supported by Association Retina France (MA), AP-HP (RF), the NIH (HCH), and the American Health Assistance Foundation (HCH). We would particularly like to thank Claude Foucher, President of Retina France; Professor Jean-François Dhainaut, President of the University René Descartes and Professor Patrick Berche, Dean of Paris V Medical School for their continuous support. We thank Fondation pour La Recherche Médicale, Fondation de l'Avenir, AFM, ARC, Ligue Nationale Contre le Cancer, Société de Secours des Amis des Sciences.

## **REFERENCES**

1. Krill, A. E., Morse, P. A., Potts, A. M., and Klien, B. A. (1966) *Am J Ophthalmol* **61**, 1405-1415
2. Ponjavic, V., Eksandh, L., Andreasson, S., Sjostrom, K., Bakall, B., Ingvast, S., Wadelius, C., and Ehinger, B. (1999) *Ophthalmic Genet* **20**, 251-257

3. Seddon, J. M., Sharma, S., Chong, S., Hutchinson, A., Allikmets, R., and Adelman, R. A. (2003) *Ophthalmology* **110**, 1724-1731
4. Cross, H. E., and Bard, L. (1974) *Am J Ophthalmol* **77**, 46-50
5. Eksandh, L., Bakall, B., Bauer, B., Wadelius, C., and Andreasson, S. (2001) *Ophthalmic Genet* **22**, 107-115
6. Palmowski, A. M., Allgayer, R., Heinemann-Vernaleken, B., Scherer, V., and Ruprecht, K. W. (2003) *Doc Ophthalmol* **106**, 145-152
7. Scholl, H. P., Schuster, A. M., Vonthein, R., and Zrenner, E. (2002) *Vision Res* **42**, 1053-1061
8. Marmorstein, A. D., Marmorstein, L. Y., Rayborn, M., Wang, X., Hollyfield, J. G., and Petrukhin, K. (2000) *Proc Natl Acad Sci USA* **97**, 12758-12763
9. Marquardt, A., Stohr, H., Passmore, L. A., Kramer, F., Rivera, A., and Weber, B. H. (1998) *Hum Mol Genet* **7**, 1517-1525
10. Petrukhin, K., Koisti, M. J., Bakall, B., Li, W., Xie, G., Marknell, T., Sandgren, O., Forsman, K., Holmgren, G., Andreasson, S., Vujic, M., Bergen, A. A., McGarty-Dugan, V., Figueroa, D., Austin, C. P., Metzker, M. L., Caskey, C. T., and Wadelius, C. (1998) *Nat Genet* **19**, 241-247
11. Stohr, H., Marquardt, A., Nanda, I., Schmid, M., and Weber, B. H. (2002) *Eur J Hum Genet* **10**, 281-284
12. Sun, H., Tsunenari, T., Yau, K. W., and Nathans, J. (2002) *Proc Natl Acad Sci USA* **99**, 4008-4013
13. Tsunenari, T., Sun, H., Williams, J., Cahill, H., Smallwood, P., Yau, K. W., and Nathans, J. (2003) *J Biol Chem* **278**, 41114-41125

14. Qu, Z., Wei, R. W., Mann, W., and Hartzell, H. C. (2003) *J Biol Chem* **278**, 49563-49572
15. Seddon, J. M., Afshari, M. A., Sharma, S., Bernstein, P. S., Chong, S., Hutchinson, A., Petrukhin, K., and Allikmets, R. (2001) *Ophthalmology* **108**, 2060-2067
16. Allikmets, R., Seddon, J. M., Bernstein, P. S., Hutchinson, A., Atkinson, A., Sharma, S., Gerrard, B., Li, W., Metzker, M. L., Wadelius, C., Caskey, C. T., Dean, M., and Petrukhin, K. (1999) *Hum Genet* **104**, 449-453
17. Kramer, F., White, K., Pauleikhoff, D., Gehrig, A., Passmore, L., Rivera, A., Rudolph, G., Kellner, U., Andrassi, M., Lorenz, B., Rohrschneider, K., Blankenagel, A., Jurklies, B., Schilling, H., Schutt, F., Holz, F. G., and Weber, B. H. (2000) *Eur J Hum Genet* **8**, 286-292
18. White, K., Marquardt, A., and Weber, B. H. (2000) *Hum Mutat* **15**, 301-308
19. Marchant, D., Gogat, K., Boutboul, S., Pequignot, M., Sternberg, C., Dureau, P., Roche, O., Uteza, Y., Hache, J. C., Puech, B., Puech, V., Dumur, V., Mouillon, M., Munier, F. L., Schorderet, D. F., Marsac, C., Dufier, J. L., and Abitbol, M. (2001) *Hum Mutat* **17**, 235
20. Izatt, J. A., Hee, M. R., Swanson, E. A., Lin, C. P., Huang, D., Schuman, J. S., Puliafito, C. A., and Fujimoto, J. G. (1994) *Arch Ophthalmol* **112**, 1584-1589
21. Hee, M. R., Izatt, J. A., Swanson, E. A., Huang, D., Schuman, J. S., Lin, C. P., Puliafito, C. A., and Fujimoto, J. G. (1995) *Arch Ophthalmol* **113**, 325-332
22. Puliafito, C. A., Hee, M. R., Lin, C. P., Reichel, E., Schuman, J. S., Duker, J. S., Izatt, J. A., Swanson, E. A., and Fujimoto, J. G. (1995) *Ophthalmology* **102**, 217-229
23. Renner, A. B., Tillack, H., Kraus, H., Kramer, F., Mohr, N., Weber, B. H., Foerster, M. H., and Kellner, U. (2005) *Ophthalmology* **112**, 586-592

24. Cartegni, L., Wang, J., Zhu, Z., Zhang, M. Q., and Krainer, A. R. (2003) *Nucleic Acids Res* **31**, 3568-3571
25. Qu, Z., Fischmeister, R., and Hartzell, C. (2004) *J Gen Physiol* **123**, 327-340
26. Kramer, F., Mohr, N., Kellner, U., Rudolph, G., and Weber, B. H. (2003) *Hum Mutat* **22**, 418
27. Qu, Z., and Hartzell, C. (2004) *J Gen Physiol* **124**, 371-382
28. Hartzell, C., Qu, Z., Putzier, I., Artinian, L., Chien, L. T., and Cui, Y. (2005) *Physiology (Bethesda)* **20**, 292-302
29. Marchant, D., Gogat, K., Dureau, P., Sainton, K., Sternberg, C., Gadin, S., Dollfus, H., Brasseur, G., Hache, J. C., Dumur, V., Puech, V., Munier, F., Schorderet, D. F., Marsac, C., Menasche, M., Dufier, J. L., and Abitbol, M. (2002) *Ophthalmic Genet* **23**, 167-174
30. McGee, T. L., Devoto, M., Ott, J., Berson, E. L., and Dryja, T. P. (1997) *Am J Hum Genet* **61**, 1059-1066
31. Vithana, E. N., Abu-Safieh, L., Allen, M. J., Carey, A., Papaioannou, M., Chakarova, C., Al-Magthteh, M., Ebenezer, N. D., Willis, C., Moore, A. T., Bird, A. C., Hunt, D. M., and Bhattacharya, S. S. (2001) *Mol Cell* **8**, 375-381
32. Esumi, N., Oshima, Y., Li, Y., Campochiaro, P. A., and Zack, D. J. (2004) *J Biol Chem* **279**, 19064-19073
33. Bakall, B., Marknell, T., Ingvast, S., Koisti, M. J., Sandgren, O., Li, W., Bergen, A. A., Andreasson, S., Rosenberg, T., Petrukhin, K., and Wadelius, C. (1999) *Hum Genet* **104**, 383-389

34. Caldwell, G. M., Kakuk, L. E., Griesinger, I. B., Simpson, S. A., Nowak, N. J., Small, K. W., Maumenee, I. H., Rosenfeld, P. J., Sieving, P. A., Shows, T. B., and Ayyagari, R. (1999) *Genomics* **58**, 98-101
35. Lotery, A. J., Munier, F. L., Fishman, G. A., Weleber, R. G., Jacobson, S. G., Affatigato, L. M., Nichols, B. E., Schorderet, D. F., Sheffield, V. C., and Stone, E. M.. (2000) *IOVS* **41**, 1291-1296

Family / Isolated case	Exon	Nucleotide change	Amino acid change	Effect	Residue at the same position in human VMD2L1/VMD2L2/VMD2L3	Conservation in RFP proteins	Hot Spot region	Putative transmembrane domain	Familial probands (n=21)	Isolated patients (n=6)	Normal subjects (n=100)
D	4	c.504C>G	L134V	-	Leu / Leu / Leu	90%	/	Between TM2 and TM3	1	/	0
F / c	6	c.652C>T	R218C*	Charge	Arg / Arg / Arg	88%	III	Between TM2 and TM3	1	1	0
A, I / a, b, f	6	c.653G>A	R218H*	hydrophobicity	Arg / Arg / Arg	88%	III	Between TM2 and TM3	1	3	0
H	6	c.665G>A	G222E	Charge	Gly / Ser / Ser	27%	III	Between TM2 and TM3	2	/	0
d	6	c.692G>C	S231T	hydrophobicity	Ser / Ser / Gly	25%	III	Between TM2 and TM3	/	1	0
e	6	c.698C>A	P233Q	Polarity	Pro / Pro / Pro	100%	III	Between TM2 and TM3	/	1	0
C	8	c.879G>C	Q293H	Charge	Gln / Gln / Gln	23%	IV	After TM4	8	/	0
B	8	c.880C>G	L294V*	-	Leu / Ile / Leu	81%	IV	After TM5	3	/	0
J	8	c.894G>A	G299R	Charge	Gly / Gly / Gly	97%	IV	After TM6	1	/	0
E	8	c.916A>G	E306G*	Charge	Glu / Glu / Glu	93%	IV	After TM7	3	/	0
G	8	c.922A>G	N308S*	-	Asn / Asn / Asn	96%	IV	After TM8	1	/	0

\* previously reported

Table 1: Mutations in the *VMD2* gene.



<b>Exon</b>	<b>Nucleotide change</b>	<b>Polymorphism</b>	<b>Individuals in this study (n=79)</b>
2	c.109T>C	L37L*	21
3	c.201G>C	L67L*	2
3	c.219C>A	I73I*	6
10	c.1410A>G	T470T*	54
10	c.1557C>T	S519S*	36
10	c.1608T>C	T536T*	39

\* previously reported

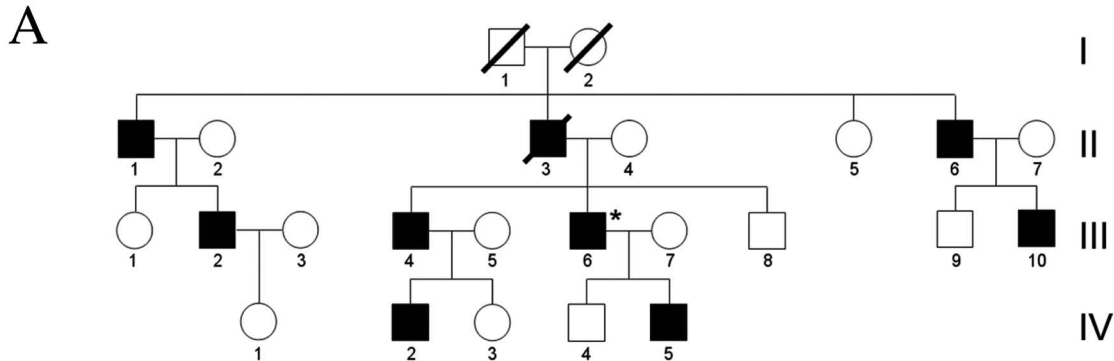
Table 2: Polymorphisms in the *VMD2* gene.

**Figure 1.** (A) Pedigree of a family affected by Best disease caused by a Gln293His mutation in the *VMD2* gene. This sequence variation was confirmed in all affected individuals by direct sequencing. (B) Heterozygous nucleotide change in codon 293 (CAG > CAC) observed in all affected patients of this family. Clinical diagnosis of BVMD by fundus examination, EOG, OCT and mERG of a 10-year-old boy (C: patient IV-5) and his father (D: patient III-6), of a 71-year-old man (E: patient II-1) and his son. (F: Patient III-2)

**Figure 2.** Whole-cell patch clamp analysis of Cl<sup>-</sup> currents induced by wild type hBest1 and the Q293H mutation. Q293H mutation blocked the normal function of hBest1 as Ca<sup>2+</sup>-activated Cl<sup>-</sup> channel in transfected HEK-293 cells. The voltage clamp protocol is shown above A. The representative current traces in A), B) and C) were from cells transfected with wild-type (WT), Q293H mutant and WT+Q293H hBest1, respectively. (D) Averaged current-voltage (*I-V*) relations for WT (n=13), Q293H (n=7), and co-transfection of WT & Q293H (n=12). (E) Current amplitudes at -100 and +100 mV from above recording were presented together with those from EGFP alone-transfected cells (n=5). Dots indicated data from individual cells. Whole-cell recording from transfected HEK-293 cells showed that Q293H mutant channel is non-functional when transfected alone, and significantly inhibited the wild-type current when cotransfected with WT hBest1 ( $p < 0.05$ , two-tailed *t* test).



# Q293H mutation in the family C



Patient	Age of onset	Age at examination	Visual acuity	EOG (Arden ratio) N > 1,8	Fundus examination	Fluorescein angiography	mfERG	OCT
II-1	< 6	71	< 20/100	1,3	Bilateral atrophy of the central macula	- Choroidal neovessel development very extensive in the right eye	Retinal electrogenesis of the central cones severely altered	- Dramatic thinning of the neurosensory retina with an epiretinal membrane-like detachment - Enhanced optical reflectivity from the choroid
III-2	5	35	20/200	1,1	Typical vitelliform lesions	Development of foveolar choroidal neovessels	Retinal electrogenesis of the central cones altered	- Flattened foveal contour - Elevation of the neurosensory retina due to a mound of highly reflective material at the RPE layer - Disruption of the photoreceptor layer
III-6	/	41	20/20	1	Normal	Normal	Normal	Normal
IV-5	5	10	20/200	1	- Bilateral vitelliform appearance - Rapid fragmentation of the lesion in the right eye	Not done	Not done	- Elevation of the macular retina due to the vitelliform lesion - Highly reflective material at the RPE layer

